

Atomic scattering factors for K-shell electron energy-loss spectroscopy

M. P. Oxley and L. J. Allen*

School of Physics, University of Melbourne, Victoria 3010, Australia. Correspondence e-mail:
 lja@physics.unimelb.edu.au

Atomic scattering factors for *K*-shell electron energy-loss spectroscopy (EELS) have been calculated for elements in the range $Z = 6$ (carbon) to $Z = 50$ (tin). The calculations are based on relativistic Hartree–Fock wave functions for the atomic bound states and Hartree–Slater wave functions for the continuum states. The results are presented in parameterized form so that accurate values of the scattering factors can be obtained for incident electron energies between 50 and 400 keV, collection semi-angles between 10 and 40 mrad, and energy windows between 25 and 100 eV. The parameterizations are for scattering vectors with magnitude $s = \sin \theta / \lambda$ up to 2.5 \AA^{-1} (2θ is the scattering angle and λ is the wavelength of the incident electrons).

© 2001 International Union of Crystallography
 Printed in Great Britain – all rights reserved

1. Introduction

Electron energy-loss spectroscopy (EELS) provides, as does energy-dispersive X-ray analysis (EDX), a means to determine the elements present in a specimen (Egerton, 1996a). EELS has advantages for the case of light elements (where X-ray fluorescence yields are low and X-ray absorption is important). For crystalline samples, ionization cross sections measured as a function of the orientation of the incident electron beam can also provide information on the sites at which specific elements are located and their concentration. This technique is known as atom location by channelling enhanced microanalysis (ALCHEMI). Formulations of ALCHEMI at various levels of approximation have been discussed by Oxley *et al.* (1999), illustrated by applications to EDX. Precisely known atomic scattering factors are essential for accurate ALCHEMI based on inner-shell EDX and must realistically model the ‘delocalization’ of the ionization interaction. Calculations using realistic atomic wave functions give excellent agreement with experiment – see for example Oxley & Allen (1998) and Oxley *et al.* (1999). Atomic scattering factors pertinent to EDX, based on *K*- and *L*-shell ionization, have recently been given in tabular and parameterized forms by Oxley & Allen (2000). The need for scattering factors which correctly model the ionization interaction is crucial for ALCHEMI based on inner-shell EELS, where the effective interactions are in general more ‘delocalized’ than in the case of EDX. The variation of the ionization cross section as a function of orientation was pointed out in the early 1980s (Stobbs & Bourdillon, 1982; Taftø & Krivanek, 1982; Taftø & Lehmpfuhl, 1982; Self & Buseck, 1983). However, these early results have not led to ALCHEMI based on EELS, mainly due to lack of theoretical tools to calculate cross sections based on realistic ionization interactions. This paper remedies that situation for *K*-shell EELS.

The atomic scattering factors presented here are also pertinent to the calculation of images obtained using scanning transmission electron microscopy (STEM) based on *K*-shell EELS (Rafferty & Pennycook, 1999; Essex *et al.*, 1999).

The atomic scattering factors in this paper and those for EDX based on inner-shell ionization (Oxley & Allen, 2000) follow a substantial number of parameterizations of elastic scattering factors for X-rays and electrons (Strand & Bonham, 1963; Doyle & Turner, 1968; Rez *et al.*, 1994; Meyer *et al.*, 1995; Waasmeier & Kirfel, 1995; Wang *et al.*, 1995; Peng *et al.*, 1996a; Su & Coppens, 1997; Peng, 1998) and for thermal diffuse scattering (TDS) of electrons (Bird & King, 1990; Peng *et al.*, 1996a,b). In this paper, atomic scattering factors for *K*-shell ionization in the context of EELS are calculated from first principles using relativistic Hartree–Fock wave functions for atomic bound states and Hartree–Slater wave functions for the continuum states. Atomic scattering factors are presented for elements in the range $Z = 6$ (carbon) to $Z = 50$ (tin). We have confined ourselves to the *K* shell, where the channelling effects needed for ALCHEMI are most pronounced and where an EELS signal is most ‘localized’. The results are presented in parameterized form so that accurate values of the scattering factors can be obtained for incident electron energies E_0 between 50 and 400 keV, collection semi-angles α between 10 and 40 mrad, and energy windows ΔE between 25 and 100 eV. The parameterizations are for scattering vectors with magnitude $s = \sin \theta / \lambda$ up to 2.5 \AA^{-1} (2θ is the scattering angle and λ is the wavelength of the incident electrons).

2. Atomic scattering factors

2.1. Theory

The general form of the atomic scattering factor for inner-shell ionization is given by (Allen & Josefsson, 1995)

$$f(\mathbf{s}, \mathbf{s}') = \frac{1}{2\pi^3 a_0^2} \int k' \kappa^2 \left\{ \int \left[\sum_{l,m_l} n_{m_l} \int F_{l,m_l}^{\beta*}(\mathbf{Q}_s, \boldsymbol{\kappa}) \right. \right. \\ \times F_{l,m_l}^{\beta}(\mathbf{Q}_{s'}, \boldsymbol{\kappa}) d\Omega_{\kappa} \left. \right] \frac{d\Omega_{\kappa'}}{|\mathbf{Q}_s|^2 |\mathbf{Q}_{s'}|^2} \right\} d\kappa, \quad (1)$$

where the scattering vector \mathbf{s} has magnitude given by $s = k \sin \theta / 2\pi$, k is the magnitude of the incident wavevector \mathbf{k} . We use the convention $k = 2\pi/\lambda$, where λ is the wavelength of the incident radiation. The relativistic Bohr radius is denoted by a_0 . The symbol k' is the magnitude of the wavevector \mathbf{k}' of the scattered electron. The wavevector of the ejected electron is denoted by $\boldsymbol{\kappa}$ (magnitude κ). The quantum number associated with orbital angular momentum is denoted by l . The sum over the azimuthal quantum number m_l of the initial bound state of the atom is required for other than s orbitals. The number of electrons in each suborbital is taken into account by the factor n_{m_l} . For EDX, the integration over the solid angle $d\Omega_{\kappa'} = \sin \theta d\theta d\phi$ extends over all space. The atomic scattering factors for EELS are calculated by limiting the integration over θ to the range specified by the collection semi-angle α . The range of integration over κ is determined by the energy window ΔE of the EELS detector. The atomic transition-matrix elements F_{l,m_l}^{β} (where β labels the atomic species) will be defined in detail below and are functions of $\mathbf{Q}_s = q + 4\pi s$, where $\hbar \mathbf{q} = \hbar(\mathbf{k} - \mathbf{k}')$ is the momentum transfer. The factor of 4π in the definition of \mathbf{Q} ensures that \mathbf{s} is similar, for example, to that in the commonly used parameterizations of elastic scattering factors of Doyle & Turner (1968).

The atomic transition-matrix element for a specific suborbital in atom species β is given by

$$F_{l,m_l}^{\beta}(\mathbf{Q}_s, \boldsymbol{\kappa}) = \int b^{\beta*}(\boldsymbol{\kappa}, \mathbf{r}) \exp[i\mathbf{Q}_s \cdot \mathbf{r}] u_0^{\beta}(\mathbf{r}) d\mathbf{r}. \quad (2)$$

Here $u_0^{\beta}(\mathbf{r})$ and $b^{\beta}(\boldsymbol{\kappa}, \mathbf{r})$ are the wave functions for the bound and continuum states, respectively. Analytic evaluations of the integral inside the square brackets in (1), for K -shell ionization in a linear momentum representation and using a screened hydrogenic model, have been presented previously (Maslen, 1983). This integral may be calculated in an angular momentum representation (Saldin & Rez, 1987; Oxley & Allen, 1998) which facilitates the use of more realistic atomic wave functions and is not limited to K -shell ionization.

The use of a central potential model results in the following form for the bound-state wave function:

$$u_0^{\beta}(\mathbf{r}) = (1/r) u_{nl}(r) Y_{lm_l}(\hat{\mathbf{r}}). \quad (3)$$

Here, $u_{nl}(r)$ denotes the radial wave function for the orbital specified by the quantum numbers n and l . We use a $\hat{\cdot}$ to denote a unit vector in the argument of the spherical harmonic $Y_{lm_l}(\hat{\mathbf{r}})$. The appropriate form of the continuum wave function is (Landau & Lifshitz, 1977)

$$b^{\beta}(\boldsymbol{\kappa}, \mathbf{r}) = \frac{1}{2\kappa r} \sum_{l'=0}^{\infty} i^{l'} (2l'+1) \exp(i\delta_{l'}) u_{kl'}(r) P_l(\hat{\boldsymbol{\kappa}} \cdot \hat{\mathbf{r}}), \quad (4)$$

where $\delta_{l'}$ is the partial wave phase shift. The continuum wave function is normalized as

$$\int b^{\beta*}(\boldsymbol{\kappa}, \mathbf{r}) b^{\beta}(\boldsymbol{\kappa}', \mathbf{r}) d\mathbf{r} = (2\pi)^3 \delta(\boldsymbol{\kappa}' - \boldsymbol{\kappa}), \quad (5)$$

with the radial wave function $u_{kl'}(r)$ satisfying

$$\int u_{kl'}(r) u_{kl'}(r) d\mathbf{r} = 2\pi \delta(\kappa' - \kappa). \quad (6)$$

$u_{kl'}(r)$ are normalized by matching the asymptotic form (Landau & Lifshitz, 1977)

$$u_{kl'}(r \rightarrow \infty) = 2 \sin[\kappa r + (1/\kappa) \log 2\kappa r - \frac{1}{2} l' \pi + \delta_{l'}] \quad (7)$$

to Coulomb functions at a suitably large radius.

Expanding the exponential term in (2) and the Legendre polynomial in (4) in terms of spherical harmonics, then (2) can be written in the form

$$F_{l,m_l}^{\beta}(\mathbf{Q}_s, \boldsymbol{\kappa}) = \frac{8\pi^2}{\kappa} \sum_{l'=0}^{\infty} \sum_{m_{l'}=-l'}^{l'} (-i)^{l'} \exp(-i\delta_{l'}) Y_{l'm_{l'}}(\hat{\boldsymbol{\kappa}}) \\ \times \sum_{\lambda=0}^{\infty} \sum_{m_{\lambda}=-\lambda}^{\lambda} i^{\lambda} Y_{\lambda m_{\lambda}}^*(\hat{\mathbf{Q}}_s) \int (1/r^2) u_{kl'}(r) j_{\lambda}(Q_s r) \\ \times u_{nl}(r) Y_{l'm_{l'}}^*(\hat{\mathbf{r}}) Y_{lm_l}(\hat{\mathbf{r}}) Y_{\lambda m_{\lambda}}(\hat{\mathbf{r}}) d\mathbf{r}, \quad (8)$$

where the index λ (not to be confused with wavelength) arises from the expansion for the exponential. Introducing the notation

$$G_{nl,kl'}^{\lambda}(Q_s) = \int u_{kl'}(r) j_{\lambda}(Q_s r) u_{nl}(r) d\mathbf{r} \quad (9)$$

and using the properties of the spherical harmonics, the atomic transition-matrix element can be written in the form

$$F_{l,m_l}^{\beta}(\mathbf{Q}_s, \boldsymbol{\kappa}) = \frac{8\pi^2}{\kappa} \sum_{l'=0}^{\infty} \sum_{m_{l'}=-l'}^{l'} (-1)^{m_{l'}} (-i)^{l'} \exp(-i\delta_{l'}) Y_{l'm_{l'}}(\hat{\boldsymbol{\kappa}}) \\ \times \sum_{\lambda=0}^{\infty} \sum_{m_{\lambda}=-\lambda}^{\lambda} i^{\lambda} Y_{\lambda m_{\lambda}}^*(\hat{\mathbf{Q}}_s) G_{nl,kl'}^{\lambda}(Q_s) \\ \times \left[\frac{(2l'+1)(2\lambda+1)(2l+1)}{4\pi} \right]^{1/2} \begin{pmatrix} l' & \lambda & l \\ 0 & 0 & 0 \end{pmatrix} \\ \times \begin{pmatrix} l' & \lambda & l \\ -m_l & m_{\lambda} & m_l \end{pmatrix}. \quad (10)$$

The arrays are Wigner $3j$ symbols.

The term in square brackets in equation (1) can now be evaluated using the orthonormality of the spherical harmonics and the orthogonality relations for the $3j$ symbols (Oxley & Allen, 1998). This yields

$$I(\mathbf{Q}_s, \mathbf{Q}_{s'}, \boldsymbol{\kappa}) = \sum_{l,m_l} n_{m_l} \int F_{l,m_l}^{\beta*}(\mathbf{Q}_s, \boldsymbol{\kappa}) F_{l,m_l}^{\beta}(\mathbf{Q}_{s'}, \boldsymbol{\kappa}) d\Omega_{\kappa} \\ = \left(\frac{4\pi}{\kappa} \right)^2 (2l+1) \sum_{l'=0}^{\infty} (2l'+1) \sum_{\lambda=0}^{\infty} (2\lambda+1) \\ \times G_{nl,kl'}^{\lambda}(Q_s) G_{nl,kl'}^{\lambda}(Q_{s'}) \begin{pmatrix} l' & \lambda & l \\ 0 & 0 & 0 \end{pmatrix}^2 \\ \times P_{\lambda}(\hat{\mathbf{Q}}_s \cdot \hat{\mathbf{Q}}_{s'}). \quad (11)$$

40 mrad is sufficient. For annular detectors, for example one spanning 20 to 30 mrad, the scattering factors for 20 mrad can be subtracted from the scattering factors for 30 mrad. Similarly to calculate the scattering factors for, for example, an energy window between 50 and 75 eV, the relevant scattering factors are subtracted.

3. Use of scattering factors to calculate ionization cross sections pertinent to ALCHEMI

The diffraction of the incident electrons in a crystalline sample makes the cross section for ionization a function of incident-beam orientation, the site of the inelastic event within the unit cell and the depth within the crystal. The phase of the atomic

transition-matrix elements is an essential part of the physics. We assume that the incident electrons are plane waves. Then a general expression, describing the cross section for inelastic scattering of electrons from a crystal of thickness t , based on the one-particle Schrödinger equation and which implicitly assumes integration over all final states of the scattered electron, is as follows (Allen & Rossouw, 1993; Allen & Josefsson, 1995, 1996):

$$\sigma = NV_c \left\{ \left[1 - \sum_{i,j} B^{ij}(t) \sum_g C_g^i C_g^{j*} \right] \mu_{0,0} + \sum_{i,j} B^{ij}(t) \sum_{g,h} C_g^i C_h^{j*} \mu_{h,g} \right\}, \quad (14)$$

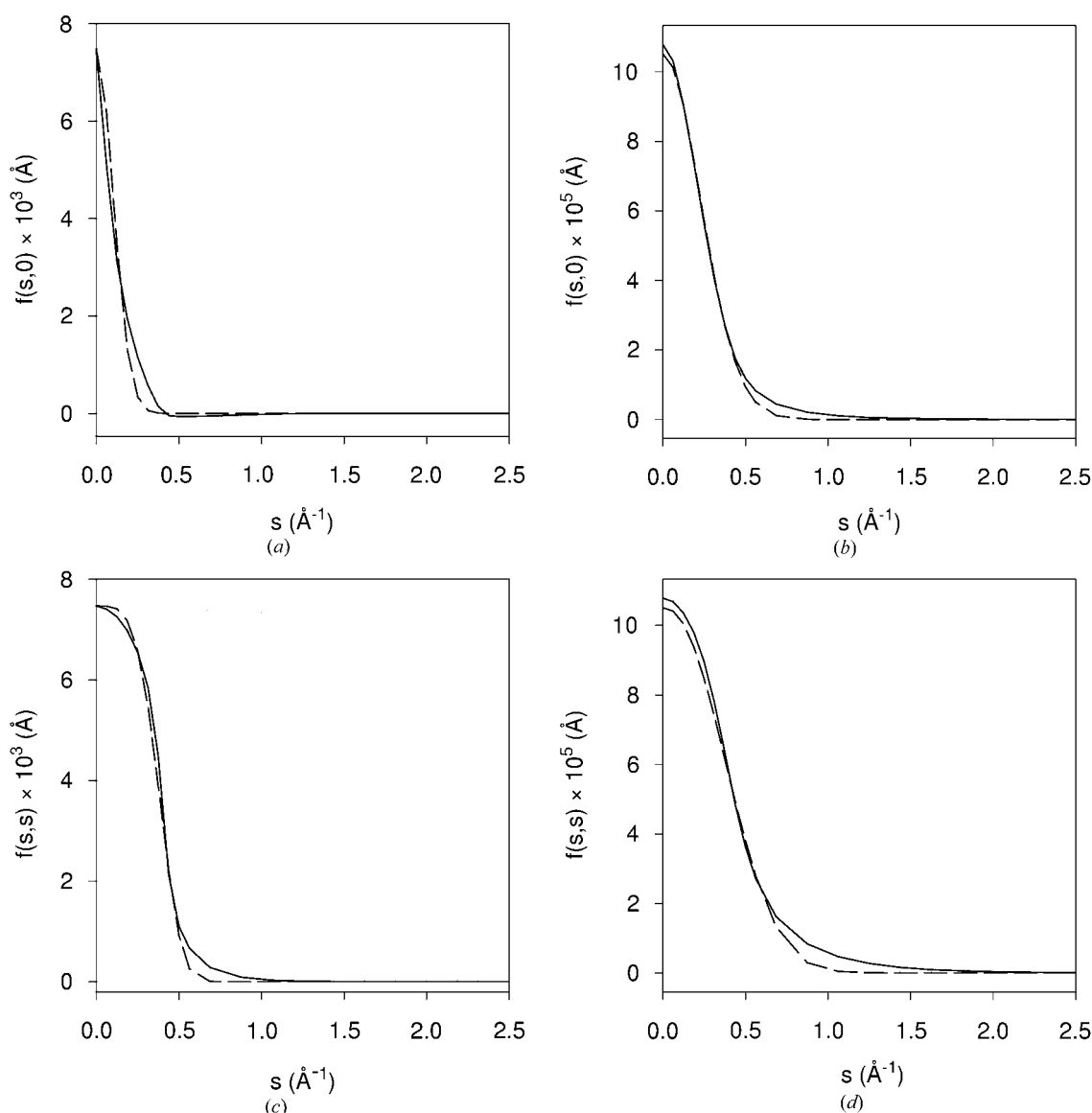


Figure 1

Atomic K -shell ionization scattering factors $f(s, 0)$ calculated for incident energy $E_0 = 100$ keV, collection semi-angle $\alpha = 30$ mrad, and energy window $\Delta E = 50$ eV for (a) carbon and (b) silicon. The results calculated from first principles are shown by the solid lines and the parameterizations, as defined in Table 1 and Table 2, by the dashed lines. The diagonal scattering factors $f(s, s)$, defined in Table 3 and Table 4, are also shown for (c) carbon and (d) silicon.

where NV_c is the total crystal volume and

$$B^{ij}(t) = \alpha^i \alpha^{j*} \frac{\exp[i(\lambda^i - \lambda^{j*})t] - 1}{i(\lambda^i - \lambda^{j*})t}. \quad (15)$$

The Bloch-wave eigenvalues λ^i in the $B^{ij}(t)$, the Bloch-state amplitudes α^i and Fourier coefficients $C_{\mathbf{g}}^i$, which represent the eigenvector of the i 'th state, come from solution of the Bethe scattering equations (Allen & Josefsson, 1995), where \mathbf{g} denotes a reciprocal-lattice vector. This result can also be

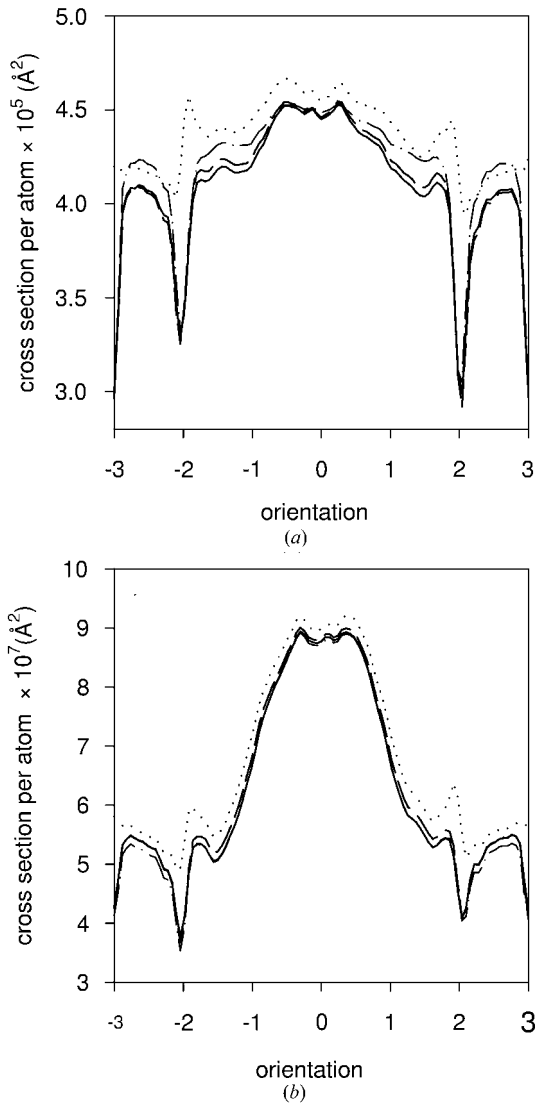


Figure 2

Cross sections for K -shell ionization by 100 keV electrons incident on a 1000 Å thick SiC crystal under {111} systematic row conditions and as a function of orientation for (a) carbon and (b) silicon. A value of unity on the orientation axis indicates that \mathbf{g}_{111} is in the exact Bragg orientation. A collection semi-angle $\alpha = 30$ mrad and energy window $\Delta E = 50$ eV have been used. Non-local calculations from first principles are shown by the solid lines and cross sections calculated in the local approximation are shown by the dotted lines. The results of calculations using the ‘mixed’ approximation are shown by the dashed lines and the same calculation using the parameterizations in Tables 1–4 is shown by the dashed-dotted lines. Absorption due to TDS is taken into account, as discussed in the text.

obtained with suitable approximations from the formalism of Dudarev *et al.* (1993). While in this paper the $\mu_{\mathbf{h},\mathbf{g}}$ describe inner-shell ionization, they may in general describe any specific inelastic scattering under consideration. It is important to note that, while the $\mu_{\mathbf{h},\mathbf{g}}$ refer to a specific form of absorptive scattering, the eigenvector components $C_{\mathbf{g}}^i$ in (14) and complex eigenvalues λ^i in (15) come from solution of the total scattering equations (Allen & Josefsson, 1995) and, hence, in principle, take into account all forms of absorptive scattering concurrently occurring. In particular, the inclusion of thermal diffuse scattering (TDS) is crucially important to obtain accurate cross sections (Allen & Rossouw, 1993; Allen & Josefsson, 1995). The first term in equation (14) (the factor in square brackets multiplied by $\mu_{0,0}$) accounts for ionization by electrons that have been ‘dechannelled’ or absorbed from the dynamical elastic beams by wide-angle (mainly TDS) scattering. The second term represents the dynamical contribution to σ (which is attenuated by the absorptive scattering). Channelling for the scattered electrons can also be taken into account (Allen, 1993; Schattschneider *et al.*, 1996). The conditions under which double channelling is important have been investigated by Josefsson & Allen (1996).

The inelastic scattering coefficients for ionization required to calculate ionization cross sections as a function of orientation of the incident beam in a particular crystal can be expressed, in terms of the atomic inner-shell ionization scattering factors (Allen & Josefsson, 1995), as

$$\mu_{\mathbf{h},\mathbf{g}} = \frac{1}{kV_c} \sum_{\beta_n} \exp[-M_{\beta}(\mathbf{g} - \mathbf{h})] \exp[i(\mathbf{g} - \mathbf{h}) \cdot \tau_{\beta_n}] \times f_{\beta}(\mathbf{h}/4\pi, \mathbf{g}/4\pi), \quad (16)$$

where \mathbf{g} and \mathbf{h} are reciprocal-lattice vectors and the vectors τ_{β_n} describe the position of each atom of type β within the unit cell and the Debye–Waller factor for atoms of type β , $M_{\beta}(\mathbf{g} - \mathbf{h}) = \frac{1}{2} |\mathbf{g} - \mathbf{h}|^2 \langle u_{\beta}^2 \rangle$, is given in terms of the projected mean-square thermal displacement $\langle u_{\beta}^2 \rangle$.

Note that the atomic scattering factors $f(s, 0)$ and $f(s, s)$ presented in this paper are such that they may need to be divided by 4π if used in conjunction with the atomic scattering factors of Doyle & Turner (1968). This statement can be understood by looking at equation (16) and noting that if we make the replacement $k \rightarrow 4\pi s$ then the factor $1/4\pi$ may be absorbed in the atomic scattering factors, as performed by Doyle & Turner, but which has not been performed here. This is also the case for the scattering factors given for EDX by Oxley & Allen (2000).

A commonly used approximation to simplify the calculation of the inelastic scattering coefficients for ionization is the so-called local approximation (Allen & Josefsson, 1995) where it is assumed $\mu_{\mathbf{h},\mathbf{g}} \approx \mu_{\mathbf{h}-\mathbf{g},0}$. For relatively ‘localized’ ionization interactions, it is sufficient to calculate the ionization cross section assuming $f(\mathbf{h}/4\pi, \mathbf{g}/4\pi) \approx f[(\mathbf{h} - \mathbf{g})/4\pi, \mathbf{0}]$ (Oxley & Allen, 2000). An important consequence of this approximation is the assumption that $\mu_{\mathbf{h},\mathbf{h}} \approx \mu_{0,0}$, *i.e.* that all diagonal elements are equal, or, equivalently, $f(\mathbf{s}, \mathbf{s})$ is independent of \mathbf{s} . For the more ‘delocalized’ interactions observed in EELS,

especially for small collection semi-angles and energy windows in light elements, this is not a good approximation. Hence the parameterization of $f(s, s)$ for $Z \leq 30$. [Remember that $f(s, s') \approx f(s, s')$ for all s and s' .]

In Fig. 1, the atomic scattering factors for K -shell ionization of carbon and silicon, calculated from first principles, are compared to the parameterized scattering factors. The scattering factors are calculated for an incident energy $E_0 = 100$ keV, with a collection semi-angle $\alpha = 30$ mrad and an energy window $\Delta E = 50$ eV. The scattering factors appropriate for use in the local approximation are shown in Figs. 1(a) and 1(b) for carbon and silicon, respectively. For carbon, $f(s, 0)$ is small but negative for $0.4 \leq s \leq 1.4 \text{ \AA}^{-1}$, as discussed in §2.2. In Figs. 1(c) and 1(d), the form of the diagonal scattering factors $f(s, s)$ are shown for carbon and silicon, respectively. It is obvious that even for small values of s around 0.5 \AA^{-1} the approximation $f(s, s) \approx f(0, 0)$ is a poor one. For lighter elements, the form of $f(s, 0)$ becomes more Lorentzian like, especially for larger collection semi-angles. This is seen in Fig. 1(a) for the carbon K shell where the parameterization underestimates the value of the scattering factor for $0.2 \leq s \leq 0.4 \text{ \AA}^{-1}$. For this reason, elements lighter than carbon have not been parameterized as the Gaussian form of (12) fails to provide a suitable fit to the scattering factors. For the silicon K shell shown in Fig. 1(c), the value of $f(0, 0)$ is slightly underestimated by the parameterization in Table 1. The overall agreement between the parameterization and the calculated result is however quite good. The scattering factor is underestimated for $0.5 \leq s \leq 1.3 \text{ \AA}^{-1}$ but in this range the calculated scattering factor is already small and this difference is not significant.

This breakdown of the local approximation has been pointed out previously (Allen & Josefsson, 1995; Allen *et al.*, 1997) and becomes more acute for smaller collection semi-angles α . The effect of this discrepancy can be seen in Fig. 2 where the ionization cross sections are calculated as a function of orientation, using a 15 beam approximation, for 100 keV electrons incident on a 1000 \AA thick slab of SiC under {111} systematic row conditions. A collection semi-angle of 30 mrad and energy window of 50 eV have been used. TDS has been included using an Einstein model (Allen & Rossouw, 1990; Bird & King, 1990) using mean square thermal displacements of $\langle \mu_\beta^2 \rangle = 0.002793 \text{ \AA}^2$ for silicon and $\langle \mu_\beta^2 \rangle = 0.002885 \text{ \AA}^2$ for carbon, which are appropriate for 300 K (Reid, 1983). The full non-local calculation produces a cross section with greater variation than that predicted by the local approximation. This is particularly the case for carbon K -shell ionization, as shown in Fig. 2(a), where the ionization interaction is very ‘delocalized’. The cross section calculated in the local approximation is also shifted upwards due to the overestimation of the diagonal elements of the scattering matrix in the local approximation. Even for the less ‘delocalized’ case of ionization of the silicon K shell, the detailed structure of the cross section is not reproduced in the local approximation and an upward shift is again obvious. To correct for this discrepancy, we introduce the ‘mixed’ approximation. Here the off-diagonal elements of the structure matrix are calculated using the

local approximation $\mu_{\mathbf{h}, \mathbf{g}} \approx \mu_{\mathbf{h}-\mathbf{g}, 0}$ and the correct non-local diagonal terms are used. The addition of the correct diagonal terms in the ionization scattering matrix results in much better agreement with the full non-local calculation with the maximum (average) discrepancy being 1.4% (0.2%) for carbon and 3.3% (1.2%) for silicon. Clearly, for ‘delocalized’ interactions, the variation of the diagonal terms of the ionization structure matrix cannot be ignored. For larger Z , $f(s, 0)$ alone suffices to calculate cross sections as a function of orientation. The cross section for the carbon K shell in the mixed approximation, calculated using the parameterized scattering factors (shown in Fig. 1), shows larger differences, mainly to the underestimation of $f(s, 0)$ between $0.2 \leq s \leq 0.4 \text{ \AA}^{-1}$. This in effect truncates the number of beams that contribute to the cross-section calculation and leads to slight loss of detailed structure. The maximum (average) discrepancy between the full non-local calculation and the cross section calculated using the parameterizations is 4.7% (2.5%). For silicon, the maximum (average) discrepancy between the full non-local calculation and the cross section calculated using the parameterizations is 6.2% (1.2%), which is mainly due to the difference between the full non-local calculation and the ‘mixed’ approximation.

An important consideration is the effect of diffraction of the scattered fast electron after ionization has occurred. For a large detector this can be shown to average to an effective plane wave (Josefsson & Allen, 1996). Therefore the use of larger apertures, between 30 and 40 mrad, is a better proposition for the calculation of accurate cross sections.

4. Conclusions

Atomic scattering scattering factors suitable for K -shell EELS have been calculated from first principles for elements in the range $Z = 6$ (carbon) to $Z = 50$ (tin). The results are presented in parameterized form such that accurate values of the scattering factors can be obtained for incident electron energies between 50 and 400 keV for collection semi-angles between 10 and 40 mrad and detector energy windows between 25 and 100 eV.

LJA acknowledges support from the Australian Research Council.

References

- Allen, L. J. (1993). *Ultramicroscopy*, **48**, 97–106.
- Allen, L. J., Bell, D. C., Josefsson, T. W., Spargo, A. E. C. & Dudarev, S. L. (1997). *Phys. Rev. B*, **56**, 9–11.
- Allen, L. J. & Josefsson, T. W. (1995). *Phys. Rev. B*, **52**, 3184–3198.
- Allen, L. J. & Josefsson, T. W. (1996). *Phys. Rev. B*, **53**, 11285–11287.
- Allen, L. J. & Rossouw, C. J. (1990). *Phys. Rev. B*, **42**, 11644–11654.
- Allen, L. J. & Rossouw, C. J. (1993). *Phys. Rev. B*, **47**, 2446–2452.
- Bird, D. M. & King, Q. A. (1990). *Acta Cryst. A* **46**, 202–208.
- Cowan, R. D. (1981). *The Theory of Atomic Structure and Spectra*. Berkeley: University of California Press.
- Doyle, P. A. & Turner, P. S. (1968). *Acta Cryst. A* **24**, 390–397.
- Dudarev, S. L., Peng, L.-M. & Whelan, M. J. (1993). *Phys. Rev. B*, **48**, 13408–13429.

- Egerton, R. F. (1996a). *Electron Energy-Loss Spectroscopy in the Electron Microscope*, 2nd ed. New York: Plenum Press.
- Egerton, R. F. (1996b). *Ultramicroscopy*, **63**, 11–13.
- Essex, D. W., Nellist, P. D. & Whelan, C. T. (1999). *Ultramicroscopy*, **80**, 183–192.
- Josefsson, T. W. & Allen, L. J. (1996). *Phys. Rev. B*, **53**, 2277–2285.
- Landau, L. D. & Lifshitz, E. M. (1977). *Quantum Mechanics*, 3rd ed. Oxford: Permagon.
- Maslen, V. W. (1983). *J. Phys. B: At. Mol. Phys.* **16**, 2065–2069.
- Meyer, H., Müller, T. & Schweig, A. (1995). *Acta Cryst. A* **51**, 171–177.
- Oxley, M. P. & Allen, L. J. (1998). *Phys. Rev. B*, **57**, 3273–3282.
- Oxley, M. P. & Allen, L. J. (2000). *Acta Cryst. A* **56**, 470–490.
- Oxley, M. P., Allen, L. J. & Rossouw, C. J. (1999). *Ultramicroscopy*, **80**, 109–124.
- Peng, L.-M. (1998). *Acta Cryst. A* **54**, 481–485.
- Peng, L.-M., Ren, G., Dudarev, S. L. & Whelan, M. J. (1996a). *Acta Cryst. A* **52**, 257–276.
- Peng, L.-M., Ren, G., Dudarev, S. L. & Whelan, M. J. (1996b). *Acta Cryst. A* **52**, 456–470.
- Rafferty, B. & Pennycook, S. J. (1999). *Ultramicroscopy*, **80**, 141–151.
- Reid, J. S. (1983). *Acta Cryst. A* **39**, 1–13.
- Rez, D., Rez, P. & Grant, I. (1994). *Acta Cryst. A* **50**, 481–497.
- Saldin, D. K. & Rez, P. (1987). *Philos. Mag. B* **55**, 481–489.
- Schattschneider, P., Nelhiebel, M., Schenner, M., Grogger, W. & Hofer, F. (1996). *J. Microsc.* **183**, 18–26.
- Self, P. G. & Buseck, P. R. (1983). *Philos. Mag. A* **48**, L21–L26.
- Stobbs, W. M. & Bourdillon, A. J. (1982). *Ultramicroscopy*, **9**, 303–306.
- Strand, T. G. & Bonham, R. A. (1963). *J. Chem. Phys.* **40**, 1686–1691.
- Su, Z. & Coppens, P. (1997). *Acta Cryst. A* **53**, 749–762.
- Taftø, J. & Krivanek, O. L. (1982). *Nucl. Instrum. Methods*, **194**, 153–158.
- Taftø, J. & Lehmpfuhl G. (1982). *Ultramicroscopy*, **7**, 287–294.
- Waasmaier, D. & Kirfel, A. (1995). *Acta Cryst. A* **51**, 416–431.
- Wang, J., Esquivel, R. O., Smith Jr., V. H. & Bunge, C. F. (1995). *Phys. Rev. A*, **51**, 3812–3818.